J. Chem Soc. Nigeria, Vol. 44, No. 1, pp 030 -040 [2019]

AQUEOUS PHASE ADSORPTION OF METANIL YELLOW ON PHOSPHORIC ACID-ACTIVATED CARBON PREPARED FROM *GMELINA ARBOREA* BARK

*B.O. Isiuku and B. I. Nwabueze

Department of Chemistry Imo State University Owerri, Nigeria

Received 11 October 2018; accepted 02 December 2018, published online 10 January 2019

ABSTRACT

Batch adsorption of Metanil Yellow on phosphoric acid-activated-carbon prepared from Gmelina arborea bark was carried out with the view to study the adsorptive capacity of the adsorbent. The Langmuir, Freundlich, Temkin isotherm models, as well as the Pseudo-first order and the Elovich kinetic models were used to simulate experimental data. Results showed that optimum equilibrium adsorption capacity, q_e, was 34.238 mg/g by initial solution concentration 100 mg/L. Equilibrium adsorption capacity increased with increase in initial dye concentration. The isotherm models used were good fits with correlation coefficients, R^2, generally above 0.98. The adsorption was controlled by liquid film diffusion. The point of zero charge pH of the carbon was 3.2. The Gibbs free energy of adsorption,(0.294, 1.369 and 2.448 kJ/mol) for initial dye concentrations (25, 50, 100 mg/L), showed non-spontaneity of the adsorption. The R_L and n (2.017) (from Freundlich model) values indicate favourable and physical process. The results show that Gmelina arborea bark is a potential precursor for activated carbon production.

Keywords: Batch adsorption, *Gmelina arborea* carbon, metanil yellow, modelling.

*Corresponding author: Tel. +2348035731300, E-mail address: obinnabisiuku@yahoo.com

INTRODUCTION

Industrial effluents contribute majorly to environmental pollution. Dyes and pigments industries are generally known to generate wastewaters with high colour, high content of organic matter, low biochemical oxygen demand (BOD) and low chemical oxygen demand (COD) [1]. These wastewaters are often discharged into the environment with or without proper treatment [2]. Visual pollution is a serious problem in water quality. It is not easy to accept red or brown water bodies [3]. In recent times, there has been a growing interest and concern over contamination of the aquatic environment by dyes. This causes reduction in the growth of algae due to obstruction of light required for photosynthesis, which subsequently leads to ecological imbalance in the aquatic ecosystem [4]. Contamination of aquatic environment by dyes has also been shown to have toxic, carcinogenic, and aesthetic effects on humans [4, 5]. Azo dyes once released into water bodies produce toxic amines by the reductive cleavage of azo linkages which cause severe effects on human beings through damaging the vital organs such as the brain, liver, kidneys and the reproductive system [6].

In an attempt to solve dye pollution problems, methods such as reverse osmosis, membrane separation, coagulation, chemical oxidation, biological treatments, photo-degradation and adsorption have been used. The most efficient method has been the adsorption process [7]. Adsorption is the concentration of a substance at the surface. The concentration at a surface is largely as a result of binding forces between atoms, molecules and ions of the adsorbate on the adsorbent surface. The adsorption process is used particularly in the case where pollutants do not undergo biological degradation, and concentration is very low [8]. Batch experiments are usually carried out to measure the effectiveness of adsorption in removing specific adsorbates, as well as to determine the maximum adsorption capacity [9].

Metanil yellow (MY) is a synthetic azo dye applied on wool, nylon, silk, paper, ink, aluminium, detergent, wood, fur, cosmetics, and as biological stain. It is hazardous when ingested and slightly hazardous when inhaled or contacts the eyes [10]. Toxicity data reveals that oral feeding or intraperitoneal and intratesticular administration of MY in animals produces testicular lesions, causing seminiferous tubules to suffer damage, reducing the rate of spermatogenesis. On oral consumption, it causes methaemoglobinaemia [11] and cyanosis [12] in humans, while skin contact results into allergic dermatitis [13]. MY also has tumour-producing effects and can also create intestinal [14] and enzymic [15] disorders in the human body. It is not mutagenic but can alter the expression of genes [16].

Activated carbon is a widely used adsorbent in the treatment of wastewater and drinking water because it has desirable physiochemical properties including good mechanical strength, chemical stability in diverse media, and large pore size distribution in addition to its extensive specific area [17]. Due to the fact that commercially available activated carbons are generally expensive, attention is currently paid to the preparation of activated carbon from agricultural by-products; they are cheap, and are derived from renewable sources [18-24].

Gmelina arborea (*G. arborea*) is a moderately sized to large deciduous tree with a straight trunk. It attains a height of 30 m or more and a diameter of up to 4.5 m. The bark is smooth, pale-ashy grey or grey to yellow with black patches and conspicuous corky circular lenticels [25]. It grows well in Nigeria and mainly used as timber, hence, generating a lot of bark as waste. The aim of this work was to convert *G. arborea* bark which is waste, and readily available in Nigeria, into activated carbon and investigate its efficiency in the removal of MY from aqueous solution by batch adsorption, thereby, creating a cleaner ecosystem.

MATERIALS AND METHODS

Adsorbate

The MY (M/s Merck, Switzerland) also called C.I. Acid yellow 36 used in this study was bought at Onitsha, Nigeria and used directly without further treatment. The structure of MY is shown in Figure 1. The stock solution was prepared by dissolving 1g dye per litre solution using distilled water. Working solution concentrations (C_o) (25 – 100 mg/L) used in the experiment, were obtained by dilution of the stock solution. 1M HNO_3 and 1M NaOH solutions were used for pH adjustments.

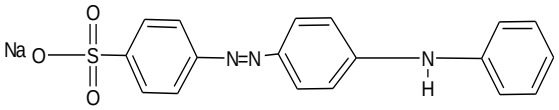

Figure 1: Structure of metanil yellow

Preparation of activated carbon

The dry *G. arborea* bark biomass obtained from the trees at Owerri, Nigeria was washed three times with distilled water and dried in the sun. The biomass was ground and soaked in 20% H_3PO_4 at a ratio 3 H_3PO_4: 1 biomass by mass for 24 h. Excess acid was removed by filtration and the biomass spread on a lattice to dry. The dry biomass was carbonized at 450 – 500^oC for 7 h. After cooling, the carbon was sieved to obtain 0.42 – 0.84 mm particle sizes and then washed with hot distilled water to a pH of about 6. The activated carbon was dried in a hot-air oven at 110^oC for 2 h, cooled and packaged in an airtight plastic container

Characterization of the activated carbon

The bulk and dry densities, and the porosity of the carbon were determined by the method of Ekpete *et al*., [26]; pore volume, by the method of Mohammed *et al*., [27]; specific surface area by the ethylene glycol monoethyl ether (EGME) method [28], Iodine number, by the Gimba and Musa method [29]; pH by the ASTM – D 3838 – 80 standard test method [30]; moisture, volatile matter, ash and fixed carbon contents by the methods of Rengaraj *et al*., [31]; AOAC [32] and Isiuku *et al*., [10] respectively. The point of zero charge pH, pH_{pzc}, was determined by the solid addition method [5]. In this method, 40 mL portions of 0.1M KNO_3 solution were introduced into eleven 100-mL conical flasks. The pH values of the solution in the flasks were adjusted to 2 – 12 with 1M HNO_3 and 1M NaOH solutions. 0.2 g portions of phosphoric acid-activated carbon (PAAC) were added into the flasks which were stoppered and put in a water-bath shaker and agitated at 125 rpm for 5 h at 30 ^oC and atmospheric pressure. The pH values of the supernatants were measured. Values of ΔpH were plotted against initial pH values. The point the plot cuts the initial pH axis is the pH_{pzc}. $\Delta pH = pH_f - pH_i$, where pH_f and pH_i are final and initial pH values**.** The surface structure of the adsorbent was examined with a scanning electron microscope (SEM model

Phenom Prox, M/s Phenom World, Netherlands).

Batch adsorption study

Batch adsorption studies were carried out by shaking 25 mL portions of MY solution of known C_o (25, 50 and 100 mg/L) with 0.02 g portions of the activated carbon in 50 mL flasks at pH 3, shaker speed 175 rpm and temperature 30 ^oC. The adsorption was run for 300 min for each initial concentration. Samples were taken after regular time intervals of 60 min, filtered and analysed with a UV - Vis spectrophotometer (Shimadzu UV – 752, M/s Shimadzu, Japan) at λ_{max} 440 nm.

The quantities of MY adsorbed per unit mass of adsorbent q_t (mg/g) at time t (min) and at equilibrium q_e (mg/g) were determined using Eqs. 1 and 2:

$$q_t(mg/g) = \frac{(C_o - C_t)V}{1000x} \quad \ldots\ldots\ldots(1)$$

$$q_e(mg/g) = \frac{(C_o - C_e)V}{1000x} \quad \ldots\ldots(2)$$

Where, C_o, C_t and C_e (mg/L) are the liquid-phase concentrations of the dye at time zero, time t (min) and at equilibrium respectively, V (cm^3) is the volume of the solution and x (g), the mass of dry adsorbent.

RESULTS AND DISCUSSION

Physicochemical properties

The physicochemical parameters of the adsorbent are shown in Table 1. Above pH 3.2 adsorption of MY will be low. This is due to the fact that the surface of the carbon was negatively charged, hence repulsion of the MY ions which are also negatively charged. This explanation is supported by the work of Akinola and Umar [5].

Effects of initial concentration and contact time

The effect of contacting 0.02 g portions of PAAC with 25 mL portions of MY solution of C_o 25, 50 and 100 mg/L is shown in Figure 2. There was sharp rise in q_e for the first 180 min with gradual rise as time elapsed. This condition arose due to the large number of vacant binding sites on the adsorbent available at the beginning of the process, which reduced with time. Supportive work had been done by Salman and Njoku [18]. Figure 2 also shows that q_e (mg/g) increased with increase in C_o. This is attributed to the increase in the concentration gradient which acts as a driving force [33].

Adsorption isotherm modelling

The distribution of the MY between the dye solution and the activated carbon surface at equilibrium is shown by an adsorption isotherm. Analysis of experimental data with various isotherm models is an important step in finding the suitable model that can be used for design purposes [34]. Adsorption isotherm is basically useful in describing the interaction between the adsorbate and the adsorbent and is critical in

optimizing the use of adsorbents. Correlation coefficient (R^2) values combined with percentage error are used to know the fitness of the model applied.

Langmuir isotherm model

The Langmuir isotherm model assumes the presence of a finite number of binding sites homogeneously distributed over the adsorbent surface presenting the same affinity for adsorption of a single layer, and with no interaction between adsorbed species [35]. The well-known Langmuir model equation [36] is expressed as Eq. 3:

$$q_e = \frac{q_o K_L C_e}{1 + K_L C_e} \quad \ldots\ldots\ldots\ldots\ldots\ldots (3)$$

Where, q_o (mg/g) is the equilibrium adsorption capacity q_e (mg/g) for a complete monolayer, K_L (L/mg) is a constant related to the affinity of the binding sites and energy of adsorption.

The linear form of Langmuir model equation is expressed as Eq. 4:

$$\frac{C_e}{q_e} = \frac{1}{q_o K_L} + \frac{C_e}{q_o} \quad \ldots\ldots\ldots\ldots\ldots\ldots (4)$$

A plot of C_e/q_e against C_e gave a straight line with slope $^1/q_o$ and the intercept $1/ (q_o K_L)$ (Figure not shown). The R^2 value (0.991) shows that the Langmuir model is a good fit for experimental data. Table 2 shows the q_o (mg/g) and K_L values.

The essential characteristics of the Langmuir model is expressed in terms of a dimensionless constant or separation factor R_L [37] expressed as Eq. 5:

$$R_L = \frac{1}{1 + K_L C_{om}} \quad \ldots\ldots\ldots\ldots\ldots\ldots (5)$$

Where, C_{om} is the maximum C_o. The value of R_L shows the type of the isotherm to be favourable if $0<R_L<1$, unfavourable if $R_L>1$, linear if $R_L = 1$, or irreversible $R_L = 0$.

In this work, the R_L value 0.25 shows that the adsorption was favourable.

Freundlich isotherm model

The Freundlich equation is empirical and based on adsorption on a heterogeneous surface. It provides no information on the monolayer adsorption capacity in contrast to the Langmuir model [38]. The heterogeneous adsorption surface of the adsorbent has unequal available sites with different energies of adsorption [39].The Freundlich model equation is expressed as Eq. 6:

$$q_e = K_F C_e^{1/n} \quad \ldots\ldots\ldots (6)$$

Where, K_F [mg/g(L/mg) $^{-1/n}$] is the Freundlich adsorption or distribution coefficient and $^1/n$, a measure of adsorption intensity or surface heterogeneity. $^1/n$ ranges between 0 and 1. The closer the value of $^1/n$ to zero, the more heterogeneous the surface of the adsorbent is.

The linear logarithmic form of the Freundlich equation is expressed as Eq. 7:

$$Inq_e = InK_F + \frac{1}{n} InC_e \ldots\ldots (7)$$

A plot of ln q_e versus ln C_e, gave a straight line with slope $^1/n$ and intercept ln K_F (Figure not shown).The correlation coefficient (R^2 = 1), shows that the Freundlich model is a very good fit for simulating experimental data. Table 2 shows the values of K_F and $^1/n$. The value n indicates the degree of nonlinearity between adsorbate concentration and adsorption as follows: n = 1 shows linear adsorption; $n < 1$ shows chemisorption, and $n > 1$ indicates physisorption. If n value ranges between 1 and 10, it indicates good and physical adsorption [40-42]. The n value in this work is 2.017, which shows the adsorption to be good and physical.

Temkin isotherm model

The Temkin isotherm [43] considers the effects of indirect adsorbate-adsorbate interaction on adsorption isotherm and assumes that heat of adsorption decreases linearly with coverage due to adsorbate-adsorbate interactions [44]. The model equation is expressed as Eq.8:

$$q_e = BIn(A_T C_e) = BInA_T + BInC_e \ldots (8)$$

$$B = \frac{RT}{b_T} \ldots\ldots\ldots\ldots\ldots\ldots\ldots (9)$$

Where, B (J/mol) is a constant related to the heat of adsorption, b_T (J/mol/K) is the Temkin isotherm constant related to the heat of adsorption, showing whether the process is exothermic or endothermic. A_T (L/g) is a constant corresponding to the maximum binding energy, R = 8.314 J/mol, the universal gas constant and T (K) the absolute temperature. A plot of q_e (mg/g) versus ln C_e, gave a straight line with slope B and intercept B ln A_T (Figure not shown). The R^2 value 0.989 shows the model fit for the adsorption process. Table 2 shows the values of B, b_T and A_T. Low values of B show weak interaction between adsorbent and adsorbate indicating physisorption [45]. Positive values of b_T show that the adsorption is endothermic [46]. Experimental results of 11.447 J/mol for B, and 219.344 J/mol/K for b_T show that the adsorption was physisorptive and endothermic.

Adsorption kinetics and mechanism

Isotherms are obtained under equilibrium conditions whereas in most adsorption processes, retention time is too short for equilibrium to be attained. Hence, information must be obtained on the time dependence of adsorption processes by carrying out process-oriented kinetic studies [47].

Pseudo-first order model

The Pseudo-first order (PFO) rate equation of Lagergren [48] is expressed as Eq.10:

$$log(q_e - q_t) = logq_o - \frac{k_1 t}{2.303} \ldots\ldots (10)$$

Where, k_1 is the PFO rate constant.

The slopes and intercepts of the straight-line plots of log ($q_e - q_t$) versus t (h) (Figure not shown) were used to determine the k_1 (h^{-1}) and the q_o (mg/g) for the various C_o values. Table 3 shows the values of q_o, k_1, R^2 and SSE for C_o 25, 50 and 100 mg/L. The experimental q_e values were found to be lower than the predicted q_o. This might be due to the fact that the time 300 min the adsorption was run was too short for equilibrium to be attained. The R^2 values (0.96, 0.941 and 0.968) for C_o (25, 50 and 100 mg/L), show the PFO kinetic model as a good fit in simulating experimental data.

Elovich kinetic model

The Elovich kinetic model which is often valid for systems in which the adsorbing surface is heterogeneous is mainly applicable to chemisorptions [26]. The model equation is expressed in the linearized logarithmic form as Eq.11:

$$q_t = \frac{1}{\beta} In(\alpha\,\beta) + \frac{1}{\beta} Int \ldots\ldots\ldots\ldots \quad (11)$$

Plots of q_t against ln t (Figure not shown) gave straight lines with slopes $^1/\beta$ and intercepts ($^1/\beta$) ln ($\alpha\beta$). α (mg/g/min) is the initial adsorption rate and β (g/mg) is related to the extent of surface coverage and the activation energy for chemisorptions. Table 3 shows α, β and R^2 values for all the C_o portraying the Elovich model suitable for analysing experimental data. β decreased with increase in C_o while for α, the reverse trend was the case.

Batch adsorption mechanism

To ascertain the mechanism that controlled the batch adsorption of MY on PAAC from *G. arborea* bark, the Boyd model was applied to analyse experimental data.

Boyd Kinetic Model

The Boyd kinetic model [49] is applied to differentiate between film diffusion and intra-particle diffusion and to identify the slowest step in the adsorption process. The Boyd model equation is expressed as Eq. 12:

$$F = 1 - \frac{6}{\pi^2} \sum_{n=1}^{\infty} \frac{1}{n^2}\, exp(-n^2 B_t) \ldots\ldots\ldots (12)$$

Where, B_t is a mathematical function of F which represents the fractional attainment of equilibrium at any time t. F is determined from Eq. 13 or 13a:

$$F = {}^{q_t}/_{q_e} \quad \ldots\ldots\ldots\ldots\ldots\ldots\ldots\ldots\ldots\ldots (13)$$

Where $q_t < q_e$, or

$$F = {}^{q_e}/_{q_t} \quad \ldots\ldots\ldots\ldots\ldots\ldots\ldots\ldots\ldots\ldots (13a)$$

Where $q_t > q_e$

Transformation and approximation in Eq.13 gives Eqs. 14 [50] and 15: [51, 52]

$$B_t = -0.4977 - In(1 - F) \quad for \quad (F > 0.85) \ldots (14)$$

$$B_t = 6.28318 - 3.2899F - 6.28318(1 - 1.0470F)^{\frac{1}{2}} \ldots (15)$$

$for\ (F \leq 0.85)$

If the plot of B_t against t (h) is linear and passes through the origin, it confirms the intra-particle

(or pore) diffusion as the rate-limiting step. If the plot is nonlinear or linear but does not pass through the origin, then liquid film diffusion is confirmed as the rate-limiting step. None of the plots (Figure not shown) passed through the origin. This confirms that liquid film diffusion was the rate-limiting step in the adsorption process.

The slope of the graph gives B called Boyd or time constant [53]. This value is expressed as Eq.16:

$$B = \frac{\pi^2 D_i}{r_o^2} \quad \ldots\ldots\ldots\ldots\ldots\ldots\ldots\ldots\ldots\ldots\ldots\ldots\ldots\ldots (16)$$

Where, D_i (cm^2/h) is the effective diffusion constant and r_o the radius of adsorbent particle. The value for r_o used in this work was 3.532 x 10^{-3} m.

Table 2 shows the value of B and D_i for the various C_o values 25, 50 and 100 mg/L.

Spontaneity of the adsorption process

The spontaneity of the adsorption process at various C_o was also determined [54] by applying Eq. 17:

$$\Delta G^o_{ads} = RTInK_D \ldots\ldots\ldots\ldots\ldots\ldots\ldots\ldots\ldots\ldots (17)$$

Where, K_D is the adsorption equilibrium constant or distribution coefficient., K_D was calculated [55] from Eq. 18:

$$K_D = \frac{(C_{ad})e}{C_e} \ldots\ldots\ldots\ldots\ldots\ldots\ldots\ldots\ldots (18)$$

Where, $(C_{ad})_e$ is the adsorbed adsorbate concentration at equilibrium. The ΔG^o_{ads} values were calculated as 0.294, 1.369 and 2.448 kJ/mol for C_o 25, 50 and 100 mg/L respectively. The adsorption was non-spontaneous for all the C_o values since the ΔG_{ads} values are positive. The energy for initiating the process might have come from the agitation at 175 rpm within the first hour.

Table 1: Physicochemical properties of PAAC derived from *G. aborea*

Parameters	Values
pH	6.0
Bulk density (g/cm^3)	0.51
Dry density (g/cm^3)	0.34
Porosity (g/cm^3)	0.79
Specific surface area (m^2/g)	454.54
Pore volume (g/cm^3)	0.019
Iodine number (mg/g)	35.74
Moisture content (%)	8.17
Volatile matter content (%)	45.45
Fixed carbon content (%)	37.23
Ash content (%)	9.15
pH_{pzc}	3.2

Table 2: Isotherm models parameters for batch adsorption of MY on PAAC from *G. arborea* at 29°C

Model	Parameter	Value
Langmuir	$q_{e,exp}$. (mg/g)	34.238
	q_o (mg/g)	49.751
	K_L (L/mg)	0.03
	ΔG_{ads} (kJ/mol)	8.830
	R^2	0.991
	SSE (%)	6.94
Freundlic	n^{-1}	0.496
	K_F [mg/g(L/mg)$^{1/n}$]	4.107
	R^2	1
Temkin	b_T (J/mol/K)	219.344
	A_T (L/g)	3.846
	B (J/mol)	11.447
	R^2	0.989

Table 3: Kinetic models parameters for the batch adsorption of MY on PAAC from *G. aborea* at 29°C

Parameters	C_o (mg/L)		
	25	50	100
$q_{e\ exp}$ (mg/g)	14.713	22.94	34.238
PFO			
q_o (mg/g)	59.294	40.427	68.272
k_1 (h^{-1})	1.232	0.946	0.916
R^2	0.96	0.941	0.968
SSE (%)	19.94	7.82	15.22
Elovich			
β (g/mg)	0.109	0.080	0.051
α (mg/gh)	10.551	19.141	26.588
R^2	0.9481	0.851	0.889
Liquid film diffusion			
k_{id}	1.218	0.95	0.917
R^2	0.9597	0.939	0.967
Boyd			
B	0.801	0.691	0.634
$D_i \times 10^{-6}$ (m^2/h)	1.012	0.873	0.801
R^2	0.845	0.945	0.939

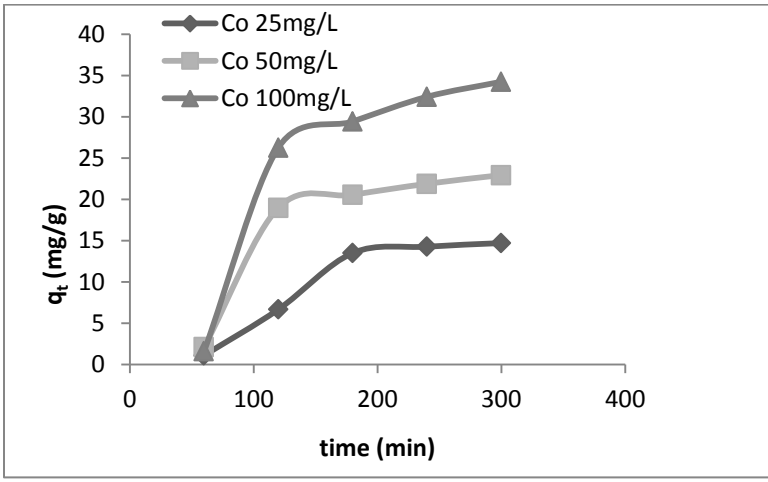

Fig. 2 : Batch adsorption of MY on PAAC derived from *G. aborea* bark at 29°C at various C_o

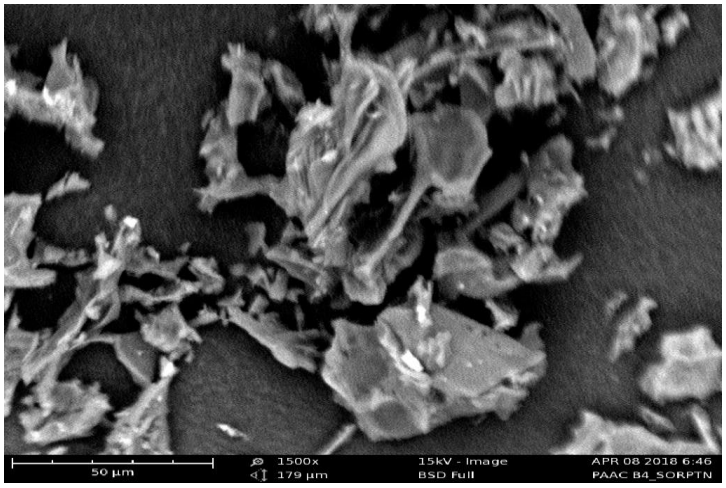

Figure 3: Scanning electron micrograph of PAAC before adsorption

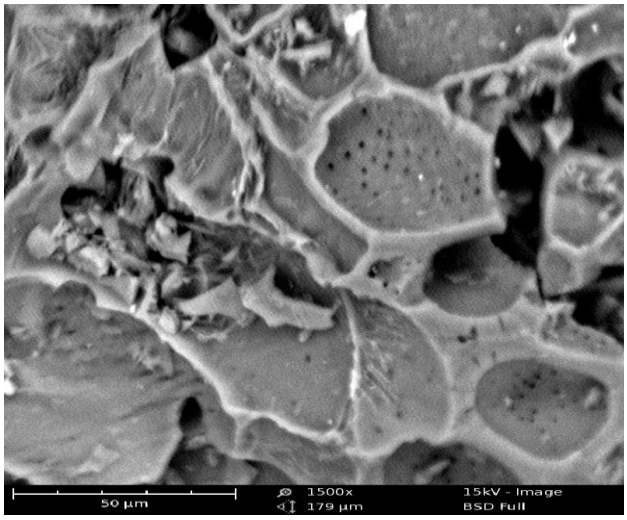

Figure 4: Scanning electron micrograph of PAAC after adsorption

CONCLUSION

PAAC was prepared from *G. arborea* bark, characterized and used to remove MY from aqueous solution by batch adsorption. Effect of C_o was studied at pH 3, temperature of 29 ^oC, adsorbent dosage 0.02 g per 25 mL solution and shaker speed 175 rpm. Experimental data show that q_e increased with increase in C_o. The optimum equilibrium adsorption capacity was 34.238 mg/g by C_o 100 mg/L.

Experimental data were analysed with Langmuir, Freundlich and Temkin isotherm models. All the models simulated experimental data well with R^2 above 0.98. However, the Freundlich model simulated experimental data best. From the values of the dimensionless factors obtained for all the C_o, the adsorption process was favourable. K_D values were applied in calculating changes in Gibb's free energy of adsorption ΔG_{ads}. The values showed that the adsorption process was non-spontaneous. The n (2.017) value in the Freundlich model, indicates that adsorption was good and physical.

Experimental data were also modelled using PFO, Elovich and kinetic models. R^2 and SSE values show PFO model the better fit. The Boyd kinetic model was used to confirm that liquid film diffusion was the rate-limiting step. PAAC from *G. aborea* bark was found to be a good adsorbent for MY removal.

REFERENCES

1. T. Tarawou, E. Young and D. Ere (2014), 'Adsorption of methylene blue dye from aqueous solution using activated carbon produced from water hyacinth in a fixed-bed column system', *Scholars Acad. J. Biosci*., 2(9): 607-612

2.A. S. Olawale, O. A. Ajayi, M. S. Olakunle, M. T. Ityokumbul and S. S. Adefila (2015), 'Preparation of phosphoric acid activated carbons from *Canarium schweinfurthii* nutshell and its role in methylene blue adsorption', *J. Chem. Eng. Mater. Sci*., 6(2): 9-14

3. A. A. Attia, W. E. Rashwan and S. A. Khedr (2006), 'Capacity of activated carbon in the removal of acid dyes subsequent to its thermal treatment', *Dyes and Pigments*, 69: 128-136

4. M. L. De Souza, P. B. De Moraes, P. R. M. Lopes, R. N. Montagnolli, D. F. De Angelis and E. D. Bidoie (2012), 'Contamination by

Remazol Red Brilliant dye and its impact in aquatic photosynthetic microbiota', *Environ. Manage. Sustainable Dev*., 1(2): 129-138

5. L. K. Akinola and A. M. Umar (2015), 'Adsorption of crystal violet onto adsorbents derived from agricultural wastes: kinetic and equilibrium studies', *J. Appl. Sci. Environ. Manage*., 19(2): 279-288
6. M. A. Oladipo, I. A. Bello, D. A. Adeoye, K. A. Abdulsalam and A. A. Giwa (2013), 'Sorptive removal of dyes from aqueous solutions: A review', *Adv. Environ. Biol*., 7 (11): 3311-3327
7. M. Auta (2012), 'Fixed-bed adsorption studies of Rhodamine B dye using oil palm empty fruits bunch activated carbon', *J. Eng. Res. Studies*, 3(3): 3-6
8. B. O. Isiuku, M. Horsfall Jnr. and A. I, Spiff (2014), 'Colour removal from a simulated Methyl Red wastewater by adsorption on carbon in a fixed bed', *Res. J. Appl. Sci*., 9(4): 201-207
9. O. B. Isiuku, M. Horsfall Jnr. and A. I. Spiff (2013), 'Adsorption of Metanil Yellow on chemically-activated carbon in a packed-bed column: Effect of activation reagent', *J. Eng. Appl. Sci*., 8 (9-12): 282-289
10. B. O. Isiuku (2015), 'Adsorption of Metanil Yellow and Methyl Red from aqueous solutions using cassava (*Manihot esculenta*) peels activated carbon in a fixed-bed column', *PhD Dissertation*, University of PortHarcourt, PortHarcourt, Nigeria
11. S. M. Sachdeva, K. V. Mani, S. K. Adval, V. P. Jolpota, K. C. Rasela and D. S. Chadha (1992), 'Acquired toxic methaemoglobinaemia', *J. Assoc. Physicians Ind.*, 40: 239-240
12. S. S. Chandro, and T. Nagaraja (1987), 'A food poisoning out-break with chemical dye: An investigation report', *Med. J. Armed Forces Ind*., 43: 293-300
13. B. M. Hausen, (1994), 'A case of allergic contact dermatitis due to Metanil Yellow', *Contact Dermatitis*, 31: 117-118
14. S. Ramachandani, M. Das, A. Joshi and S. K. Khanna (1997), 'Effect of oral and parental administration of Metanil Yellow on some hepatic and intestinal biochemical parameters', *J. Appl. Toxicol*., 17: 85-91
15. M. Das, S. Ramachandani, R. K. Upreti and S. K. Khanna (1997), 'Metanil Yellow: a bifunctional inducer of hepatic phase I and phase II xenoblastic-metabolizing enzymes', *Food Chem. Toxicol*., 35: (1997) 835-838
16. S. Gupta, M. Sundarrajan and K. V. K. Rao (2003), 'Tumor promotion by Metanil Yellow and Malachite Green during rat hepatocarcinogenesis associated with disregulated expression of cell cycle regulatory proteins', *Tertogon, Carcin. (Mut. Suppl. I)* 301-312
17. H. Zhu, X. Yang, Y. Mao, Y. Cheng, X. Long and W. Yuan (2011), 'Adsorption of

EDTA on activated carbon from aqueous solutions, *J. Hazard. Mater*., 185: 951-957

18. J. M. Salman, V. O. Njoku and B. H. Hameed (2011), 'Adsorption of pesticides from aqueous solution onto banana stalk activated carbon', *Chem. Eng, J*., 174: 33-40
19. L. Ren, J. Zhang, Y. Li and C. Zhang (2011), 'Preparation and evaluation of cattail fibre-based activated carbon for 2, 4, 6-trichlorophenol removal', *Chem. Eng. J*., 168: 553 – 561
20. W. Li, J. Zhang, C. Zhang, Y. Wang and Y. Li (2010), 'Adsorptive removal of Cr (VI) by Fe-modified activated carbon prepared from *Trapa natans* husk', *Chem. Eng. J*., 162: 667 – 684
21. B. Petrov, T. Budinova, B. Tsyntasarski, V. Kochkodan, Z. Shkavro and N. Petrov (2010), 'Removal of aromatic hydrocarbons from water by activated carbon from apricot stones', *Chem. Eng. J*., 165: 258 – 264
22. Y. Sun and P. A. Webley (2010), 'Preparation of activated carbon from corncob with large specific surface area by a variety of chemical activators and their application in gas storage', *Chem. Eng. J*., 162: 883 – 892
23. H. Dolas, O. Sahin, C. Saka and H. Demir, (2011), 'A new method in producing high surface area activated carbon: the effect of salt on the surface area and the pore size distribution of activated carbon prepared from pistachio shell', *Chem. Eng. J*., 166: 191 – 197
24. R. Baccar, P, Blanquez, J. Bouzid, M. Feki and M. Sarra (2010), 'Equilibrium, thermodynamic and kinetic studies on adsorption of commercial dye by activated carbon derived from olive-waste cake', *Chem. Eng. J*., 165: 457 – 464
25. C. Orwa, A. Mutua, R. Kindt, R. Jamnadass and R. Anthony (2009), *Agroforestree Database*: a tree reference and selection guide version 4.0 (http://www.worldagroforestry.org/sites/treedatabases.asp)
26. O. A. Ekpete (2012), 'Adsorption and kinetic studies of phenol and 2 – chlorophenol onto fluted pumpkin (Telfairia Occidentalis, Hook) stem waste activated carbon', *PhD Dissertation*, University of PortHarcourt, PortHarcourt, Nigeria
27. A. Mohammed, A. A. Aboje, M. Auta and M. Jibril, (2012), 'Comparative analysis and characterization of animal bones as adsorbent', *Adv. Appl. Sci. Res*., 3(5): 3089 - 3096
28. A. B. Cerator and A. J. Lutenegar (2002), 'Determination of surface area of fine grained soils by the ethylene glycol monoethylether (EGME) method', *J. Geotech. Testing*., 25(3): 1 -7
29. C. Gimba and I. Musa (2005), 'Adsorption of phenol and some toxic metals from textile effluent', *Proceedings of the 28th Annual*

International conference of Chemical Society of Nigeria, 32: 167 – 170

30. American Society for Testing and Materials, *Annual Book of ASTM Standard*. Vol. 15.01, 'Refractories, Carbon and Graphic Products; Activated Carbon', ASTM, Philadelphia, PA, 1996
31. S. Rengaraj, M. Seung-Hyeon and S. Sivabam (2002), 'Agricultural Solid waste for the removal of orgranics: adsorption of phenol from water and wastewater by palm seed coat activated carbon', *Waste Manage*., 22: 543 – 548
32. Association of Official Analytical Chemists (AOAC) **www.aoac.org/ISPAM/pdf/3.5%20SMPR%20Guideline%20v12.1.pdf,(2010)** assessed on 13th February, 2012
33. V. O. Njoku, C. Obi, E. E. Oguzie, A. A. Ayuk and O. S. Bello (2012), 'Removal of Cr (III) and Zn (II) from aqueous solutions by a Nigerian natural clay', *Int. J. Chem*., 22 (1): 57 – 65
34. I. A. W. Tan, A. L. Ahmad and B. H. Hameed (2008), 'Adsorption of basic dye using activated carbon prepared from oil palm shell: Batch and fixed-bed studies', 225: 13 – 28, doi:10.1016/J. *Desal*. 2007.07.005
35. S. F. Montanher, E. A. Oliveira and M. C. Rollenberg (2005), 'Removal of metal ions from aqueous solutions by sorption onto rice bran', *J. Hazard. Mater*., B117: 207 – 211
36. R. Han, W. Zou, W. Yu, S. Cheng, Y. Wang and J. Shie (2007), 'Biosorption of Methylene Blue from aqueous solution by fallen phoenix tree leaves', *J. Hazard. Mater*., 141: 156 – 162
37. M. R. H. Mas Haris and K. Sathasivam (2009), 'The removal of Methyl Red from aqueous solution using banana pseudo fibres', *Amer. J. Appl. Sci*., 6(9): 1690 - 1700
38. Z. Aksu and J. Yener (2001), 'A comparative adsorption/ biosorption study of mono-chlorinated phenols onto various sorbents', *Waste Manage*., 21: 695 -702
39. A. L. Ahmad, S. Sumathi and B. H. Hameed (2005), 'Adsorption of residue oil from palm oil mill effluent using powder and flake chitosan: Equilibrium and kinetic studies', *Water Res*., 39: 2483 – 2494
40. A. H. Al-fatlawi and M. W. Neamah (2015), 'Batch experiment and adsorption isotherm of phosphate removal by using drinking water treatment sludge and red mud', *Intl. J. Adv. Res. Sci. Eng. Technol*., 2 (3): 557-571
41. G. McKay, M. S. Otterburn and A. G. Sweeney (1980), 'The removal of colour from eluent using various adsorbents, III, Silica: Rate process', *Water Res*., 14 (1): 15-20
42. A. Ozer and H. B. Pirinc (2006), 'The adsorption of Cd (II) ions on sulphuric acid-

treated wheat bran', *J. Hazard. Mater*., 137 (2): 849-855

43. M. J. Temkin. and V. Pyzhev (1940), 'Recent modification to Langmuir isotherms', *Acta Physiochim*., USSR, 12: 217
44. V. O. Njoku, A. A. Ayuk, E. E. Oguzie, E. N. Ejike (2012), 'Biosorption of Cd(II) from aqueous solution by cocoa pod husk biomass: Equilibrium, kinetic and thermodynamic studies'. *Sep. Sci. Technol*., 47: 753-761
45. G. Nechifor, M. Pascu, G. A. Traistaru and P. C, Albu (2015), Comparative study of Temkin and Flory-Huggins isotherms for the adsorption of phosphate anion on membranes, *U. P. G. Sci. Bull. Series B,* 77 (2): 63-72
46. R. Sivakumar, and S. Arivoli (2017), 'A study on the removal characteristics of Malachite Green dye from waste water by low-cost nanoporous adsorbent', *Chemical Science Transactions*, 6 (1): 159-172
47. M. Horsfall Jnr. and A. I. Spiff (2005), 'Effects of temperature on the sorption of Pb^{2+} and Cd^{2+} from aqueous solution by caladium bicolor (wild cocoyam) biomass', *Electron. J. Biotechnol*., 8(2): 162 – 169
48. B. Koumanova, P. Peeva, S. J. Allen, K. A. Gallagher and M. G. Healy (2002), 'Biosorption from aqueous solutions by eggshell membrane and *Rhizopus oryzae*: Equilibrium and Kinetic studies', *J. Chem. Technol. Biotechnol.,* 77: 539 – 545
49. G. E. Boyd, A. W. Adamson and L. S. Myers (1947), 'The exchange adsorption of ions from aqueous solutions by organic zeolites: II. Kinetics', *J. Amer. Chem. Soc*., 69: 2836 – 2848
50. V. O. Njoku and B. H. Hameed (2011), 'Preparation and characterization of activated carbon from corncob by chemical activation with H_3PO_4 for 2,4-dichlorophenoxyacetic acid adsorption', *Chem. Eng. J.,* 173: 391 – 399
51. D. Reichenberg (1953), 'Properties of ion exchangers resins in relations to their structures, III: Kinetics of exchange', *J. Am. Chem. Soc*., 75: 589 – 598
52. K. Porkodi and K. K. Vasanth (2006), 'Equilibrium, kinetics and mechanism modeling and simulation of basic and acid dyes sorption onto jute fibre carbon: Eosine yellow, malachite green and crystal violet single component systems', *J. Hazard. Mater.,* doi:10,1016/j.jhazmat.2006.09.029
53. A. Mittal, V. K. Gupta, A. Malviya and J. Mittal (2008), 'Process development for the batch and bulk removal and recovery of a hazardous water-soluble azo dye (Metanil Yellow) by adsorption over waste materials (Bottom Ash and De-oiled Soya)', *J. Hazard. Mater.,* 151: 821 -832
54. T. Depci, A. L. Kul, Y. Onal, E. Disli, S. Z. Alkan and Z. F. Turkmenoglu (2012),

'Adsorption of Crystal Violet from aqueous solution on activated carbon derived from Gölbasi Llignite', *Physicochem. Probl. Miner. Process*, 48(1): 253-270

55. V. O. Njoku (2014), 'Biosorption potential of cocoa pod husk for the removal of Zn (II) from aqueous phase', *J. Environ. Chem. Eng*., 2: 881 – 887